JOURNAL

OF THE AMERICAN CHEMICAL SOCIETY

VOLUME 110, NUMBER 10 MAY 11, 1988

Macrochelate Complexes of Purine 5′-Nucleotide Triphosphates and Monophosphates: Definitive Multinuclear NMR Evidence Supported by Molecular Mechanics Calculations

Michael D. Reily, Trevor W. Hambley,† and Luigi G. Marzilli*

Contribution from the Department of Chemistry, Emory University, Atlanta, Georgia 30322.
Received February 12, 1987

Abstract: Historically, there has been much speculation over the existence and biological role of macrochelate metal complexes of 5′-ATP and other purine 5′-nucleotide triphosphates (5′-NTPs). In this report, we present conclusive evidence that, in dilute (5–30 mM) neutral D_2O solutions, the preferred 1:1 complexes formed between *cis*-Pt$(ND_2CH_3)_2(D_2O)_2$ and purine 5′-NTPs are monomeric macrochelates of the type *cis*-Pt$(ND_2CH_3)_2$(5′-NTP-*N7*,γP*O*) where the nucleotide is bound via N7 and an O of the γ-phosphate group. Such species were observed as intermediates during the course of the reaction when r(Pt/NTP) = 0.5 and were the major products formed at $2 \geq r \geq 1$. For 5′-ATP, the additional reactive site at N1 leads to ^{1}H NMR spectra indicative of polymerization when $r \geq 1$. The 1:1 stoichiometry of the complexes was established by the observation of two widely separated CH_3 signals each integrating to approximately 3 protons relative to the H8 signal. The observation of a *Pt concentration-independent equilibrium*

$$cis\text{-Pt}(ND_2CH_3)_2(5'\text{-ITP-}N7,\gamma PO) + Br^- \rightleftarrows cis\text{-Pt}(ND_2CH_3)_2(5'\text{-ITP-}N7)Br$$

in the presence of 100 mM KBr for 2 to 20 mM Pt concentrations is consistent only with *monomeric* species. No intermediates were observed in the formation of the bromo complex, a result consistent with a monomeric species and difficult to rationalize if the species were dimeric. Several observations support γ-phosphate binding in the macrochelates. First, ^{31}P and {^{1}H}–^{31}P NMR spectra reveal that the γP signal is 3–5 ppm downfield (depending on pH) to that of unreacted 5′-NTP. Second, the position of this downfield-shifted signal is nearly invariant in the pH range 5–8, whereas the γP signals for 5′-ITP and for *cis*-Pt$(ND_2CH_3)_2$(5′-ITP-*N7*)$_2$ both shift 6 ppm (pK_{app} ca. 6.9) over this pH range. Third, for the 5′-ITP macrochelate, the values of $^3J_{4'5'}$ and $^3J_{5'P}$ indicate an almost exclusive preference for the gauche–gauche conformations about the C4′–C5′ and the C5′–O5′ bonds. An extraordinarily large value of 3.2 Hz for $^4J_{4'P}$ strongly supports this conformational preference. A detailed analysis of the ribose coupling constants of the macrochelate indicates that it is flexible enough to maintain a normal N ⇄ S equilibrium blend of sugar ring conformations with a slight shift toward the N conformer. Molecular mechanics calculations on the model, *cis*-Pt$(NH_3)_2$(5′-GTP-*N7*,γP*O*), demonstrated that these results are consistent with γ-phosphate coordination. A similar examination of the macrochelate formed with 5′-dIMP, where only the α-phosphate group is available for coordination, revealed even more pronounced spectral effects indicating that the sugar ring clearly adopts an unusual conformation. Consistent with the observed ribose coupling constants, molecular mechanics calculations on *cis*-Pt$(NH_3)_2$(5′-GMP-*N7*,α*PO*) indicate the lowest energy N conformation (C1′-endo/C2′-exo twist) is ca. 5 kJ lower than the lowest energy S conformation, i.e., there is an 89 to 11 preference for the N conformer over the S conformer.

The widely used anticancer drug *cis*-Pt$(NH_3)_2Cl_2$ may function by interacting with the guanine and/or adenine bases of DNA.[1-3] As a consequence, nucleoside and nucleotide complexes of the drug and its analogues containing the *cis*-PtA_2 moiety, where A = amine, have been studied in depth.[4-20] Nucleotide monophosphates (NMPs) may be viewed as the simplest models for studying drug DNA interactions. However, the very rich chemistry of nucleotide species has confounded a complete elucidation of all the complexes formed with guanine or adenine 5′-NMPs, i.e., 5′-GMP and 5′-AMP. Many published studies on Pt drug binding to 5′-NMPs[14-17] have required correction and amplification (see below).[8,18-20]

† Permanent Address: School of Chemistry, University of Sydney, Sydney, N.S.W. 2006, Australia.

(1) Pinto, A. L.; Lippard, S J. *Biochim. Biophys. Acta* **1985**, *780*, 167.
(2) Ciccarelli, R. B.; Soloman, M. J.; Varshavsky, A.; Lippard, S. J. *Biochemistry* **1985**, *24*, 7533. Sundquist, W. I.; Lippard, S. J.; Stollar, B. D. *Biochemistry* **1986**, *25*, 1520. Roberts, J. J. *Adv. Inorg. Biochem.* **1981**, *3*, 273. Fichtinger-Schepman, A. M. J.; van der Veer, J. L.; den Hartog, J. H. J.; Lohman, P.; Reedijk, J. *Biochemistry* **1985**, *24*, 707.
(3) Reedijk, J.; Fichtinger-Schepman, A. M. J.; vanOosterom, A. T.; van de Putte, P. *Struct. Bonding* **1987**, *67*, 53.
(4) Marzilli, L. G. *Prog. Inorg. Chem.* **1977**, *23*, 255. Marzilli, L. G. *Adv. Inorg. Biochem.* **1981**, *3*, 47. See also: Gellert, R. W.; Bau, R. *Met. Ions Biol. Syst.*, **1979**, *8*, 1. Martin, R. B.; Miriam, Y. H. *Met. Ions Biol. Syst.* **1979**, *8*, 57.

0002-7863/88/1510-2999$01.50/0

It is now evident that the phosphate group of 5′-NMPs rarely interacts directly with Pt(II) centers.[20] However, we recently defined conditions for the formation of *cis*-PtA_2(5′-NMP-*N7*,*αPO*)[21] from *cis*-PtA_2(5′-NMP-*N7*)(H_2O) type complexes where N = G(5′-GMP) or I(5′-inosine monophosphate).[20] The formation of such *N7*,*αPO* chelates is both kinetically and thermodynamically unfavorable under most conditions.[20] For example, it appears essential to have an excess of *cis*-PtA_2 reactant over 5′-NMP to prevent formation of *cis*-PtA_2(5′-NMP-*N7*)$_2$ type complexes; once formed, *cis*-PtA_2(5′-NMP-*N7*)(H_2O) reacts readily with a second 5′-NMP to give the bis complex.[20] Of course, in the presence of an excess of 5′-NMP, the bis complex is favored.[6-12,18-20] Indeed, it is just such bis adducts, in which two bases on the same strand of DNA are bound to Pt, that are the major adducts formed on treating DNA with Pt anticancer drugs.[1,2]

Spectral characterization of *cis*-PtA_2(5′-GMP-*N7*)$_2$ complexes has laid a helpful foundation for characterizing Pt-anticancer drug adducts of oligonucleotides.[3] In contrast to typical *cis*-PtA_2(5′-GMP-*N7*)$_2$ complexes, we recently found that *cis*-PtA_2(5′-AMP-*N7*)$_2$ compounds exhibit restricted rotation about the Pt–N7 bonds and exist as a pair of head-to-tail isomers in approximately equal amounts.[19] Restricted rotation of 5′-AMP[19] could be attributed to the greater steric bulk of the 6-amino group in 5′-AMP versus the 6-oxo group in 5′-GMP. Several ^1H NMR spectral trends in our studies were consistent with previously established principles for differentiating complexes containing one nucleotide from those containing two.[8,9,18-20] Also, the ^{31}P chemical shift of the coordinated purine 5′-NMP changed little for exclusive *N7* coordination but was greatly altered (ca. 3.5 ppm) for *N7*,*αPO* coordination.[20]

While our two studies were in press, a study of the products of the reactions of *cis*-$Pt(NH_3)_2Cl_2$ with 5′-AMP, 5′-ADP, and 5′-ATP in the presence of an *excess* of NXP (N = A, X = M, D, or T) was reported.[16] A similar type of product was obtained which existed in two forms of nearly equal concentration, i.e., two similar H8 signals. However, the conclusion reached in that study was that 1:1 Pt:5′-AXP complexes were formed and that both N7 and a phosphate group bind to Pt. A very small shift (<1 ppm) of the ^{31}P signals was ascribed to direct phosphate group binding. A second study which appeared at about the same time concluded that the products were bis adducts of the type *cis*-PtA_2(5′-ATP-*N7*)(5′-ATP-*PO*).[17] This conclusion was also based on small ^{31}P shifts.

We feel that the NMR data in these two other studies [16,17] are actually for *cis*-PtA_2(5′-AXP-*N7*)$_2$ compounds and that the two H8 signals are due to restricted rotation.[19] However, these studies raised an interesting question to be posed below.

The interaction of *cis*-PtA_2 species with 5′-NDPs and 5′-NTPs has very little, if any, relevance to anticancer activity. However, the metabolic importance of metal-5′-NTP complexes, particularly for 5′-ATP, has inspired numerous investigations into the structure of 5′-NTP complexes with biologically relevant labile metal ions.[4,22-28] Such studies, aimed at understanding the relationship between structure and function, have often provided good evidence for formation of macrochelates, i.e., species where one or more phosphate groups and a base N, usually N7 of a purine, are both bound directly to the metal.[23,28] The lability of the metal centers has precluded a definitive evaluation of the ligating groups. From molecular models, it is likely that at least two groups must be bound to cis coordination positions in macrochelates. We wondered the following: Can the application of the principles which appear to have resulted in rational procedures for favoring the formation of specific *cis*-PtA_2 adducts with purine 5′-NMPs be brought to bear on this longstanding purine 5′-NTP macrochelate problem?

Since the nature of the complexes involving coordination of both purine and phosphate groups to the same metal has been the subject of much speculation and since such a species has not been characterized by X-ray crystallography,[22] we have carried out molecular mechanics calculations to evaluate chelates in which the metal is bound to N7 of a 6-oxopurine and an α, β, or γ phosphate group.

Experimental Section

Nucleotides were purchased from Sigma and used without further purification. *cis*-$Pt(ND_2CH_3)_2I_2$ was prepared by the following modification of the method of Dhara:[29] A solution of $K_2[PtI_4]$ was prepared in D_2O then cooled to 5 °C in an ice bath. The appropriate amount of 40% NH_2CH_3 was then added and the solution was warmed to ca. 50 °C and maintained at this temperature until the orange crystals stopped forming. Solutions of 40 to 100 mM *cis*-$Pt(ND_2CH_3)_2(D_2O)_2$ were prepared by suspending appropriate amounts of the iodide complex in 99.8% D_2O containing 1.95 equiv of $AgNO_3$ and stirring vigorously for ca. 10 h. After removal of the AgI, the solutions were stored in tightly closed vials at 5 °C in the dark (pH 3–4). Fresh Pt solutions were prepared at least every 4 days.

^1H NMR spectroscopy was performed on a Nicolet 360-MHz spectrometer. Spectra were recorded on samples dissolved in 99.8% D_2O with the following parameters: 7.1 μs (90°) pulse, presaturation of HDO, 16K data points, quadrature phase mode. Reported chemical shifts were made to reflect shifts from trimethylsilyl propionate (at pH 7) by setting the signal from internal tetramethylammonium nitrate (TMA) to 3.186 ppm. Reactions were normally carried out in 5-mm NMR tubes and in all cases reported pH values were obtained directly from the NMR sample with use of a 0.3 mm × 20 cm pH electrode (Ingold) and are uncorrected meter readings. In some cases we employed 0.01 M K_2HPO_4 as a buffer.

^{31}P NMR spectroscopy was performed at 81 MHz on an IBM WP200-SY spectrometer. Spectra were either recorded with a 45° pulse, 2-s repetition time or with a 90° pulse, 15-s repetition time. All spectra were recorded in the quadrature phase mode with 2 to 4 data points per hertz in the real time domain. $\{^1H\}$–^{31}P and ^{31}P NMR spectra represent the accumulation of 100 to 1000 and 1000 to 5000 transients, respectively. For the latter, the broad-band ^1H decoupling coil was greater during acquisition. In some cases, 0.01 M PIPES buffer was used.

Molecular Mechanics. The strain energy of the molecule was described as the sum of bond length deformation (E_b), valence angle deformation (E_θ), torsion angle deformation (E_ϕ), out-of-plane deformation (E_δ), nonbonded interaction (E_{nb}), electrostatic interaction (E_ϵ), and hydrogen bond interaction (E_{hb}) terms:

$$E_{total} = \sum E_b + \sum E_\theta + \sum E_\phi + \sum E_\delta + \sum E_{nb} + \sum E_\epsilon + \sum E_{hb}$$

(5) See: Martin, R. B. *Acc. Chem. Res.* **1985**, *18*, 32 and references cited therein.
(6) Marcelis, A. T. M.; Erkelens, C.; Reedijk, J. *Inorg. Chim. Acta* **1984**, *91*, 129. Marcelis, A. T. M.; van Kralinger, C. G.; Reedijk, J. *J. Inorg. Biochem.* **1980**, *13*, 213.
(7) Mansy, S.; Chu, G. Y. H.; Duncan, R. E.; Tobias, R. S. *J. Am. Chem. Soc.* **1978**, *100*, 593. Also see: Chu, G. Y. H.; Tobias, R. S. *J. Am. Chem. Soc.* **1976**, *98*, 2646.
(8) Dijt, F. J.; Canters, G. W.; denHartog, J. H. J.; Marcelis, A. T. M.; Reedijk, J. *J. Am. Chem. Soc.* **1984**, *106*, 3644.
(9) Marcelis, A. T. M.; van Kralingen, C. G.; Reedijk, J. *J. Inorg. Biochem.* **1980**, *13*, 213.
(10) Cramer, R. E.; Dahlstrom, P. L. *J. Am. Chem. Soc.* **1979**, *101*, 3679.
(11) Marcelis, A. T. M.; Korte, H.-J.; Krebs, B.; Reedijk, J. *Inorg. Chem.* **1982**, *21*, 4059.
(12) Marcelis, A. T. M.; van der Veer, J. L.; Reedijk, J.; Zwetsloot, J. C. M. *Inorg. Chim. Acta* **1983**, *78*, 195. See also: Marcelis, A. T. M. Ph.D. Thesis, University of Leiden, 1982.
(13) Eapen, S.; Green, M.; Ismail, I. M. *J. Inorg. Biochem.* **1985**, *24*, 233. Inagaki, K.; Kuwayama, M.; Kidani, Y. *J. Inorg. Biochem.* **1982**, *16*, 59.
(14) Fanchiang, Y.-T. *J. Chem. Soc., Dalton Trans.* **1986**, 135.
(15) Clore, G. M.; Gronenborn, A. M. *J. Am. Chem. Soc.* **1982**, *104*, 1364.
(16) Bose, R. M.; Cornelius, R. D.; Viola, R. E. *J. Am. Chem. Soc.* **1986**, *108*, 4403.
(17) Sarrazin, M.; Pegrot, V.; Briand, C. *Inorg. Chim. Acta* **1986**, *124*, 87.
(18) Miller, S. K.; Marzilli, L. G. *Inorg. Chem.* **1985**, *24*, 2421.
(19) Reily, M. D.; Marzilli, L. G. *J. Am. Chem. Soc.* **1986**, *108*, 6785.
(20) Reily, M. D.; Marzilli, L. G. *J. Am. Chem. Soc.* **1986**, *108*, 8299.
(21) On presenting structural formulas, the coordinating atoms in a ligand will be indicated by italics. Charges of complexes will ordinarily be omitted because these can depend on pH.
(22) Saenger, W. *Principles of Nucleic Acid Structure*; Springer-Verlag: New York, 1984.
(23) Scheller, K. H.; Hofstetter, F.; Mitchell, P. R.; Prijs, B.; Sigel, H. *J. Am. Chem. Soc.* **1981**, *103*, 247.
(24) Scheller, K. H.; Sigel, H. *J. Am. Chem. Soc.* **1983**, *105*, 5891.
(25) Yohannes, P. G.; Mertes, M. P.; Mertes, K. B. *J. Am. Chem. Soc.* **1985**, *107*, 8288 and references therein.
(26) Led, J. J. *J. Am. Chem. Soc.* **1985**, *107*, 6755.
(27) Sabat, M.; Cini, R.; Harmony, T.; Sundaralingam, M. *Biochemistry* **1985**, *24*, 7828.
(28) Mariam, Y. H.; Martin, R. B. *Inorg. Chim. Acta* **1979**, *35*, 23.
(29) Dhara, S. C. *Indian J. Chem.* **1970**, *8*, 193.

Table I. ^1H and ^{31}P NMR Spectral Data for Complexes of 5′-NTP and Reaction Products with *cis*-$Pt(NH_2CH_3)_2(H_2O)_2$

		δ ^1H[a]				δ ^{31}P[b]		
species	pH	H8	H2	H1′[c]	Me	α	β	γ[d]
5′-ITP	7.4	8.52	8.24	6.16		−14.0	−24.4	−9.1
I-I	7.4	9.07	8.29	6.22	2.51	*e*	*e*	−9.0
					2.19			
*I*Br-I	7.6	9.01	8.27	6.20	2.53			
					2.28			
II-I	6.3	8.94	8.22	6.09	2.33	−13.7	−24.0	−9.0
III-I	7.4	8.95	8.29	6.24	2.52	−13.8	−25.4	−5.4
					2.20			
5′-ATP	6.0	8.52	8.24	6.14		−14.2	−25.4	−13.0
I-A	6.0	9.24	8.32	6.26	2.51	*e*	*e*	*e*
					2.18			
II-A	6.0	9.4	8.21	6.09	2.37	*e*	*e*	*e*
		9.55	8.22	6.17	2.34			
III-A	6.0	9.16	8.36	6.27	2.53	*e*	*e*	−6.0
					2.17			

[a] 361-MHz data; chemical shifts reported relative to TSP. [b] 81.01-MHz data; chemical shifts reported relative to internal TMP. [c] In all cases a doublet was observed for H1′. See Table II for selected coupling constant data. [d] Assigned by comparison of ^{31}P and $\{^1H\}$–^{31}P spectra. [e] Signals are only slightly shifted and are obscured by those of the parent purine 5′-NTP.

The force field used was based on the all atom force field for proteins and nucleic acids reported by Weiner et al.[30] Buckingham potentials, with parameters suggested by Allinger,[31] were used to model nonbonded interactions rather than Lennard-Jones potentials employed by Weiner et al.[30] Electrostatic charges were included only for atoms involved in hydrogen bonds since the influence of metal coordination on the charges of the purine and phosphate is not known. Modification and extension of the force field was necessary to model the interaction of the metal with the nucleotide. Coordination of the purine base to platinum results in small changes in bond lengths and angles. The force field was adjusted to reproduce the geometries observed in the complexes $[Na_2(5'\text{-IMPH})_2\cdot 16H_2O]_{0.14}[Na_2(cis\text{-}Pt(NH_3)_2(5'\text{-IMP-}N7)_2)\cdot {}^{15}/_{16}H_2O]_{0.86}$,[32] *cis*-$[Pt(NH_3)_2(9\text{-ethylguanine-}N7)_2]^{2+}$,[33] and *cis*-$[Pt(NH_3)_2(\text{guanosine-}N7)_2]^{2+}$.[34] The force constant used for the platinum-to-nitrogen bond was that derived by normal coordinate analysis of the tetraammine complex.[35] The undeformed bond lengths were adjusted to reproduce the bond lengths in the complexes listed above. Modelling the platinum to phosphate oxygen interaction presented more of a problem: only one crystallographically characterized platinum(II)-to-nucleotide phosphate oxygen bond has been reported and the precision of that determination was low.[36] It appears that the Pt–O bond length is similar to the Pt–N(H_3) bond length and comparison with complexes of cobalt(III) suggests a 0.02–0.03 Å shorter bond distance for the former. Therefore, the undeformed bond was set to give a bond distance 0.03 Å shorter than the Pt–N(H_3) distance and the force constant for the latter bond was used. This modelling of the platinum-to-oxygen interaction is clearly an approximation. However, it is unlikely to be greatly wrong and, in any case, is not likely to be a significant source of error. Valence angle deformation functions involving platinum were treated in the same manner as reported previously for cobalt(III) compounds.[37] 1,3-nonbonding interactions between ligating atoms were included and coplanarity of the platinum and the ligating atoms was maintained by use of out-of-plane deformation terms.

The total energy (E_{total}) was minimized by Newton-Raphson techniques using a program described elsewhere.[38] All minimizations were continued until the largest shift in a Cartesian coordinate was less than 0.001 Å. Constraints on internal coordinates were applied using the method of Lagrangian multipliers.[38]

The model for the phosphate bound nucleotide complexes was derived from ones in which the phosphate was hydrogen bonded to an aquo ligand. The Pt–O(P) separation was gradually reduced by constraining the distance at progressively smaller values until a sensible bond length was reached.

Two degrees of conformational freedom were investigated: the conformation of the furanose ring, whether N or S, and the relative orientations of the purine base and the furanose ring, whether syn or anti.[39-42] Barriers to interconversion from one conformational form to another were also estimated by minimizing the strain energy with one torsion angle (the reaction coordinate) constrained at various values intermediate between those of the two extreme conformations.

Results

Identification of Products of Reactions with 5′-ITP and 5′-ATP. In the following presentation, we will refer to complicated ^1H NMR spectral changes associated with nucleotide binding to aquated *cis*-$Pt(ND_2CH_3)_2$. To describe these changes clearly, we will first state our assignments of the species formed and then present our reasoning. We have strong evidence for three species formed in purine 5′-NTP reactions: *cis*-$Pt(ND_2CH_3)_2$(5′-NTP-*N7*)(D_2O), *I*-N; *cis*-$Pt(ND_2CH_3)_2$(5′-NTP-*N7*)$_2$, *II*-N; and *cis*-$Pt(ND_2CH_3)$(5′-NTP-*N7*,γ-P*O*), *III*-N (where N = I or A). At pHs >6, the monoaqua species (*I*-N) are metastable whereas the bis nucleotide (*II*-N) and macrochelate species (*III*-N) are stable. Additionally, the hydroxo, chloro and bromo derivatives of *I*-N are designated as *I*OH-N, *I*Cl-N, and *I*Br-N, respectively. Since the chemical shift of the base protons for most of these complexes is dependent on pH, the H1′ signals were also used to distinguish between species. Furthermore, since N1 of 5′-ITP is relatively unreactive, we will describe our results with 5′-ITP and then those with 5′-ATP. For the time periods employed, no significant exchange of H8 occurs at these temperatures and pH values.

5′-ITP Complexes. The characteristic ^1H and ^{31}P NMR signals of 5′-ITP and some of its complexes with *cis*-$Pt(ND_2CH_3)_2$ are listed in Table I. Upon incubation of 5′-ITP with aquated *cis*-

(30) Weiner, S. J.; Kollman, P. A.; Nguyen, D. T.; Case, D. A. *J. Comput. Chem.* **1986**, *7*, 230.
(31) Allinger, N. L. *Adv. Phys. Org. Chem.* **1976**, *13*, 1.
(32) Kistenmacher, T. J.; Chiang, C. C.; Chalilpoyil, P.; Marzilli, L. G. *J. Am. Chem. Soc.* **1979**, *101*, 1143.
(33) Schollorn, H.; Raudaschl-Sieber, G.; Müller, G.; Thewalt, U.; Lippert, B. *J. Am. Chem. Soc.* **1985**, *107*, 5932.
(34) Cramer, R. E.; Dahlstrom, P. L.; Seu, M. J. T.; Norton, T.; Kashiuragi, M. *Inorg. Chem.* **1980**, *19*, 148.
(35) Schmidt, K. H.; Müller, A. *Inorg. Chem.* **1975**, *14*, 2183.
(36) Louie, S.; Bau, R. *J. Am. Chem. Soc.* **1977**, *99*, 3874.
(37) Hambley, T. W.; Hawkins, C. J.; Palmer, J. A.; Snow, M. R. *Aust. J. Chem.* **1981**, *34*, 45.
(38) Hambley, T. W. *J. Comput. Chem.*, in press.
(39) Altona, C.; Sundaralingam, M. *J. Am. Chem. Soc.* **1972**, *94*, 8205. Altona, C.; Sundaralingam, M. *J. Am. Chem. Soc.* **1973**, *95*, 2333.
(40) Altona, C. *Recl. Trav. Chim. Pays-Bas* **1982**, *101*, 413.
(41) Sarma, R. H., Ed. *Nucleic Acid Geometry and Dynamics*; Pergamon Press: New York, 1980; Chapter 1.
(42) The concept of pseudorotation is based on the following formula that interrelates the torsional angles, τ_i, in an equilateral five-member ring to the amplitude of pucker, τ_m, and the "pseudorotation angle", *P*: $\tau_i = \tau_m \cos [P + 4\pi(i-2)/5)]$ (i = 0, 1, 2, 3, 4). For a given τ_m (X-ray crystal structures reveal that τ_m values generally range from 35 to 45°[39]) the exact conformation of the five-membered ring is given by a single parameter, *P*. In classical notation, the twist configurations 3′endo-2′exo ($^3_2$T) and 2′endo-3′exo ($^2_3$T) correspond to P = 180 and 0°, respectively. All configurations with P = 0 ± 90° are of the N (for north) type; all those with P = 180 ± 90° are of the S type. Nearly all crystal structures of nucleic acid constituents fall within two *P* ranges: 0–18° (N types) and 144–180° (S types). In analyzing the ^1H–^1H and ^{31}P–^1H coupling constants to determine the ribose phosphate conformation in solution, it is usually not possible to determine discrete conformations since interchange between two or more different conformers with similar energy occurs rapidly on the NMR time scale. The torsion angle C8–N9–C1′–O4′, χ, defines the two broad classes of conformers. The syn conformers have the purine ring over the ribose ring and χ has values of 180 ± 90°. The anti conformers have the purine ring remote from the ribose and χ has values of 0 ± 90°.

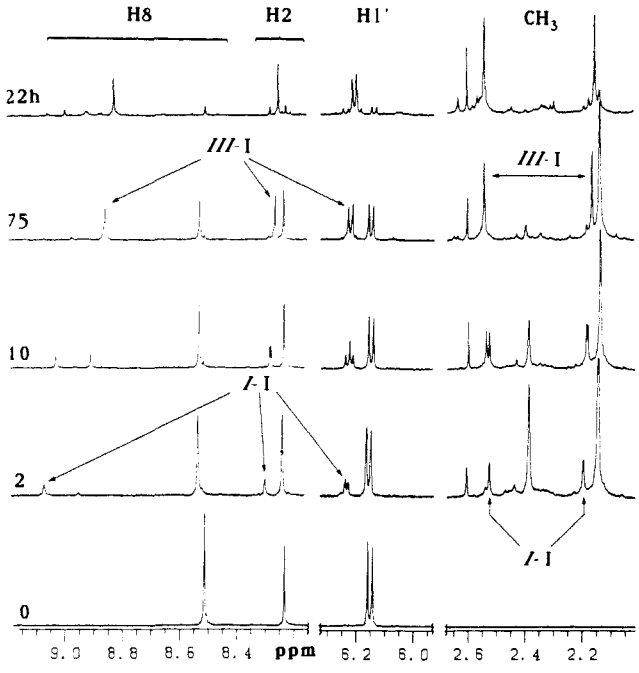

Figure 1. Time dependence of selected regions of the ^1H NMR spectrum of a mixture of 20 mM 5′-ITP and 20 mM *cis*-$Pt(ND_2CH_3)_2(OD_2)(OD)$ at initial pH 7.3, 25 °C. Spectra were recorded on samples dissolved in 99.8% D_2O at times (min) indicated after the addition of Pt solution. Slight upfield shifts of H8 and H2 over time indicate an increase in pH (final pH 7.7). See text for spectral assignments and conditions.

$Pt(ND_2CH_3)_2$ (25 °C, 2 min, r(Pt/NTP) = 1, pH 7.3), two new sets of signals are observed (Figure 1). These two sets are assigned to the monoaqua species *I*-I (downfield H8 and H1′) and the macrochelate *III*-I (upfield H8 and H1′). The chemical shift relationships of the base and H1′ signals to those of unreacted 5′-ITP (Table I) are characteristic of *N7*-bound monomeric adducts.[8,9,18,19] In addition to the signal from unreacted *cis*-$Pt(ND_2CH_3)_2(D_2O)_2$ at 2.131 ppm, the methyl region contains signals for *I*-I at 2.515 and 2.186 ppm for *III*-I at 2.534 and 2.164 ppm (Figure 1). Two signals are consistent with one nitrogen and one oxygen ligand cis to the ND_2CH_3 groups on Pt.[18] For both complexes, the Me signals each integrate to ca. three protons relative to H8, indicating a 1:1 stoichiometry (see Figure 1). At early stages of the reaction, *I*-I is the predominant complex, but after 10 min, *III*-I predominates and becomes the major final product. No intermediates between these two species are detected.

An identical reaction followed by $\{^1H\}$–^{31}P NMR spectroscopy reveals that the monoaqua *I*-I γP signal appears at −9.0 ppm (ca. 0.1 ppm downfield from the γP signal from 5′-ITP). In contrast, a highly deshielded doublet attributable to the macrochelate *III*-I appears well downfield at −5.4 ppm.

The corresponding coupled ^{31}P NMR spectrum (Figure 2, top trace) unequivocally established that this −5.4 ppm signal is from a γP since this signal is clearly not coupled to H. Furthermore, a large $^4J_{4'\alpha P}$ is observed for the macrochelate *III*-I (Supplementary Material). The αP signal from 5′-ITP itself clearly shows a much smaller ^4J interaction (Supplementary Material, Figure 2, bottom inset). The deshielded doublet from the γP of *III*-I shifts downfield less than 0.5 ppm on changing the pH from 4.8 to 8.2. This insensitivity to pH changes can be understood only if the γPO_4 group is coordinated to Pt.

When an identical reaction was carried out at pH 5.8, where γ-phosphate protonation of 5′-ITP is nearly complete, ^1H NMR spectral changes similar to those described above for the reaction at pH 7.3 were observed in the early stages of the reaction. After 11 min, however, the appearance of a third species (*II*-I) with H8 at 8.950 and H1′ at 6.10 ppm was observed. This species predominated in the reaction mixture after 22 h. A species with identical ^1H NMR signals was the only species formed when similar reactions were carried out at r = 0.5. The single Me

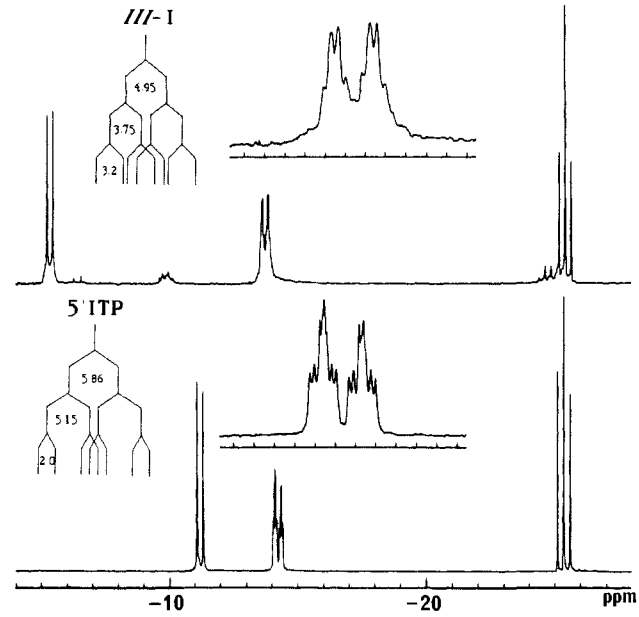

Figure 2. ^{31}P NMR spectra of 20 mM 5′-ITP (lower trace) at pH 6.8 and 20 mM *cis*-$Pt(ND_2CH_3)_2$(5′-ITP-*N7*,γP*O*) (upper trace) at pH 7.3. The insets show expansions of the αP signal region and coupling schemes. See text for spectral conditions.

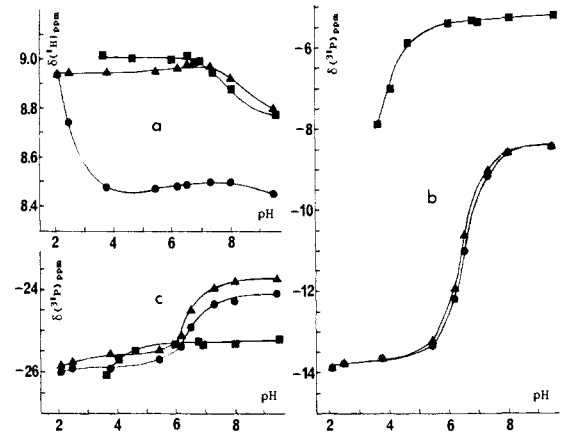

Figure 3. The pH dependence of the H8 (a) and the γ- (b) and β- (c) $\{^1H\}$–^{31}P NMR signals for 5′-ITP and various Pt derivatives: ■, *III*-I; ▲, *II*-I; ●, 5′-ITP. The pH values were recorded in D_2O and are not corrected. See text for solution conditions, spectral conditions, and methods.

resonance for this species appeared at 2.33 ppm and integrated to ca. 3 protons relative to H8. This finding is consistent with *II*-I being a bisnucleotide complex where the two 5′-ITP's are in rapid rotation about Pt–N7 bonds. The shielding of the H1′ signal of *II*-I compared with that of the mononucleotide adducts *I*-I and *III*-I is consistent with the assignment of *II*-I to a bis complex.[8,9,18,19]

The pH dependence of the H8 and phosphate NMR signals of several species is shown in Figure 3. The values for 5′-ITP and *II*-I were measured from one reaction mixture (r = 0.33, pH 6.2). *III*-I was prepared as above (r = 1, pH 7.3). Both solutions were allowed to sit at ambient temperature for 48 h after mixing, sufficient $NaNO_3$ was added to make the solutions 100 mM in this salt, and the initial spectra were recorded. The large shift of the H8 signal of 5′-ITP with apparent pK_a, pK_{app}, of ca. 2 is indicative of N7 protonation.[18] In contrast, the largest shifts of the H8 signals of the bisnucleotide *II*-I and macrochelate *III*-I species occur at higher pH and are attributable to N1 deprotonation[18] (pK_{app} ca. 8.4 and 7.9, respectively). Unlike the ^1H NMR spectral changes, the changes in the $\{^1H\}$–^{31}P NMR spectra for *II*-I and 5′-ITP are similar with pK_{app} of 6.8 (Figure 3b,c). For 5′-NTPs, γ-PO_4 group pK_a's are generally ca. 7.4–7.6.[22]

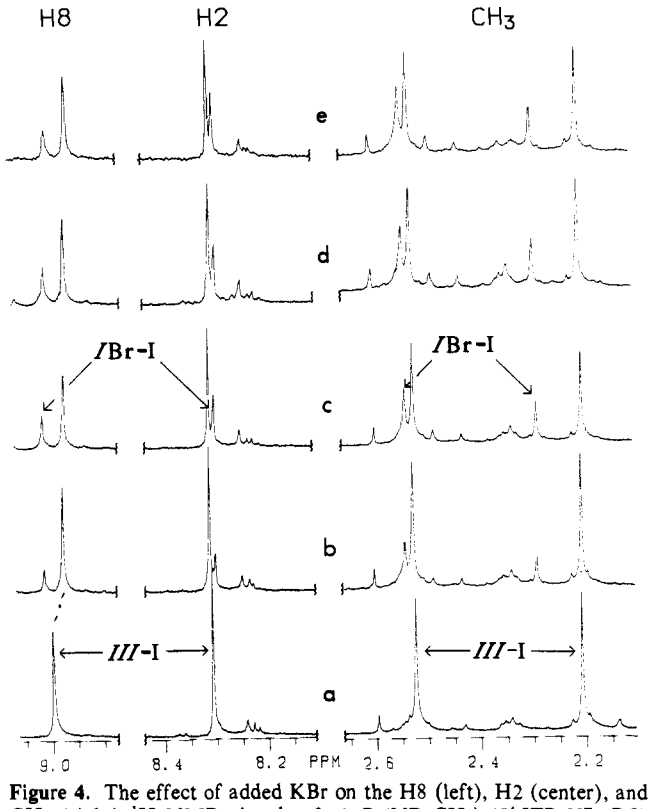

Figure 4. The effect of added KBr on the H8 (left), H2 (center), and CH_3 (right) ^1H NMR signals of *cis*-$Pt(ND_2CH_3)_2$(5'-ITP-*N7*,γ*PO*) (*III-I*) (25 °C): (a) 20 mM *III*-I, pH 7.2. Traces b–d were recorded at the following times after addition of 100 mM KBr to the above solution: (b) 5 h; (c) 27 h; and (d) 51 h. (e) 10 mM *III*-I, pH 7.2, after incubation with 100 mM KBr for 52 h, 25 °C. No detectable changes were observed in these solutions after sitting 5 days at 25 °C. See text for spectral conditions.

Although the data are not complete due to loss of *III*-I at pH <3.6, this complex clearly has a low pK_{app}. The Pt–OP bond in the macrochelate is unstable under these low pH conditions, as found previously for purine 5'-NMP macrochelates.[20]

Addition of 100 mM KBr to a solution of ca. 20 mM in *III*-I (pH 7.3, 25 °C) resulted in the slow appearance ($t_{1/2} \cong 5$ h) of one species, *I*Br-I (Figure 4). Spectral changes ceased after ca. 27 h; after 51 h, the H8 signal for *I*Br-I accounted for 31% of the total H8 area for *I*Br-I and *III*-I. In an identical experiment, except where [*III*-I] ≅ 10 mM, very similar changes were observed (Figure 4, top trace). After 52 h, deconvolution of the H8 signal area for *I*Br-I and *III*-I indicated that the percentages of these two species were 27% and 73%, respectively. If *III*-I were actually a dimer, we should observe an intermediate dimer with one coordinated Br, and an increase in the relative intensity of the H8 signal of *I*Br-I at equilibrium when the initial concentration of *III*-I was halved. In a similar experiment at pH 7.7, the relative equilibrium amounts of *I*Br-I at 2 and 20 mM total Pt concentrations were identical. If *III*-I were a dimer, a three-fold greater amount of *I*Br-I would have been observed.

5'-ATP Complexes. The ^1H NMR spectra of 5'-ATP solutions incubated with various ratios of Pt (22 h, 40 °C, pH 6) are shown in Figure 5. At high *r* values, the broad features and loss of signal intensity strongly suggest that N1-bound and possibly polymeric species are important. At lower *r* values, signals assignable to the bisnucleotide *II*-A and/or the macrochelate *III*-A are observed.

When *r* = 0.5 (ambient temperature, pH 6) two species were observed at short times with H8 signals at 9.24 and 9.16 ppm and H1' signals at 6.27 and 6.26 ppm, respectively (Figure 6). By analogy to the ITP system and $\{^1H\}$–^{31}P NMR spectra (see below), we assign these two species to the monoaqua *I*-A and the macrochelate *III*-A, respectively (see Table I). The species with the upfield H8 signal (*III*-A) is identical with the major species in an "equilibrated" reaction mixture when *r* = 1 (Figure 5, middle trace).

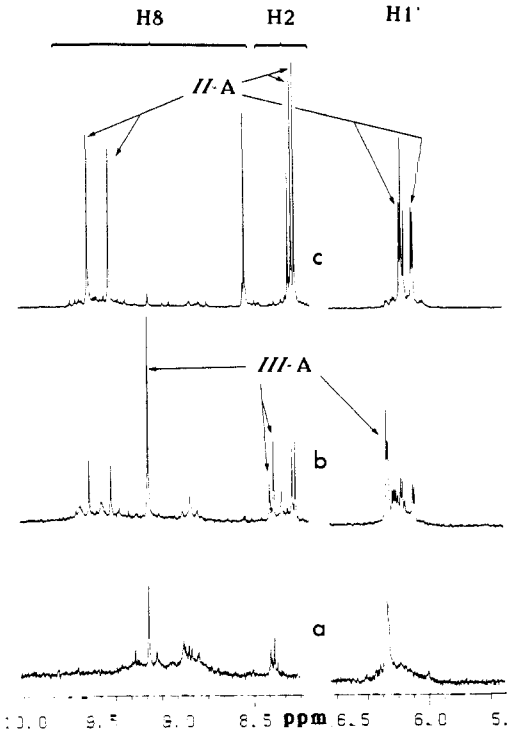

Figure 5. H8 and H1' region of "equilibrated" mixtures of 5'-ATP (10 mM) and *cis*-$Pt(ND_2CH_3)_2(OD_2)(OD)$ at pH 6.4. Solutions were warmed at 40 °C for 20 h. (a) Pt/ATP *r* = 2.0, (b) *r* = 1.0, (c) *r* = 0.5. See text for spectral conditions and assignments.

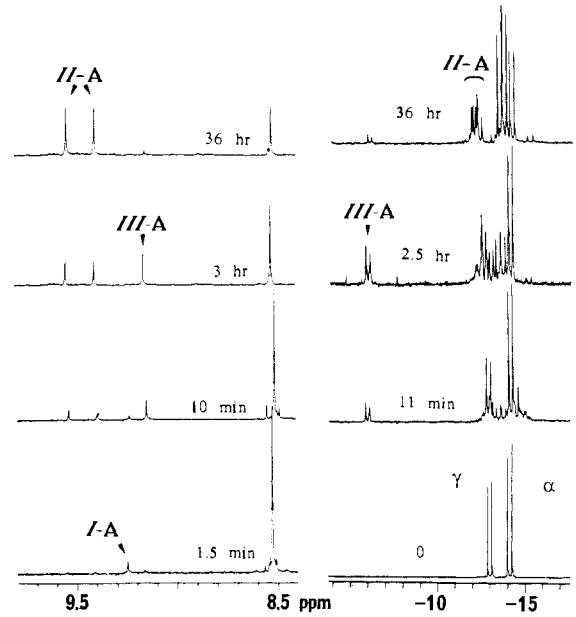

Figure 6. Time dependence of the H8 (left) and the γ and α $\{^1H\}$–^{31}P (right) NMR signals of mixtures of 20 mM 5'-ATP and 10 mM *cis*-$Pt(ND_2CH_3)_2(OD_2)(OD)$, pH 6.0. Spectra recorded at the times indicated. Solutions were in 99.8% D_2O buffered with K_2HPO_4 (^1H NMR) or PIPES (^{31}P NMR).

After 10 min, a pair of signals appeared with H8 at 9.41 and 9.55 ppm and H1' at 6.09 and 6.18 ppm; these signals predominated at long times (Figure 6, top left trace). The relative areas of the two sets of signals are nearly equal and were invariant over the course of the reaction. The corresponding Me signals for these species are at 2.34 and 2.38 ppm and each integrates to ca. 3 protons relative to H8, indicative of a bis species.[18,19] In addition, the H2 and H1' signals are shielded relative to unreacted nucleotide (Table I); indeed, the changes in the ^1H chemical shifts for *II*-A, relative to unreacted nucleotide, are quite similar to those reported for *cis*-$Pt(ND_3)_2$(5'-AMP-*N7*)$_2$.[19] Furthermore, the Me

signals for *cis*-$Pt(ND_2CH_3)_2$(5′-AMP-*N7*)$_2$ appear at 2.35 and 2.39 ppm.[19] If these species contained bound phosphate groups, the Me signals should have very different chemical shifts. The small difference in shift observed (0.04 ppm) is consistent with head-to-tail rotamers in slow exchange for *cis*-$Pt(ND_2CH_3)_2$-(5′-AMP-*N7*)$_2$ and *II*-A. However, the two H8 signals for II-A showed no sign of coalescence up to 70 °C, which indicates a greater barrier to rotation about the Pt–N7 bond for the 5′-ATP complex compared to the 5′-AMP complex.[19]

The $\{^1H\}$–^{31}P NMR spectral changes on a sample identical with that described above (r = 0.5) are shown in Figure 6. From its time course, the highly deshielded doublet at −6.0 ppm clearly arises from the same species we assign to the macrochelate *III*-A in the ^1H NMR spectra in Figure 6. Both *I*-A and *II*-A, the monoaqua and bisnucleotide species, respectively, exhibit coordination shifts of less than 0.5 ppm for all ^{31}P signals relative to 5′-ATP.

Addition of 0.10 M Cl^- to an "equilibrated" reaction mixture (r = 1.0) caused the appearance of two new H8 signals at 9.15 and 9.19 ppm which increased with time ($t_{1/2} \cong$ 36 h at 25 °C). A concomitant decrease in the signal from *III*-A is consistent with the formation of *I*Cl-A from *III*-A with the former in slow rotation. The H8 signals assigned to bisnucleotide complex *II*-A are not affected by the added Cl^-.

"Mixed" Reactions. Addition of 0.5 equiv each of 5′-ATP and 5′-ITP to a solution of *cis*-$Pt(ND_2CH_3)_2(D_2O)_2$ (20 mM), followed by incubation at 25 °C, pH 6 for 36 h, led to a solution with $\{^1H\}$–^{31}P signals at −5.3 and −6.4 ppm characteristic of *III*-I and *III*-A, respectively. No other signals were observed in this deshielded region. The ^1H NMR spectrum also revealed no signals that could not be assigned to signals observed in the individual reactions. These findings are most easily understood if *III*-I and *III*-A are both monomeric macrochelates since more complex spectra would have resulted from the presence of mixed dimers. Such mixed dimers should form since the hypoxanthine and adenine bases have virtually identical sizes and the basicity of the γ-phosphate group should be essentially identical in *I*-I and *I*-A.

Comparison of Chelates Involving α or γ PO Coordination: NMR Studies. The signals of the ribose protons of 5′-ITP and the macrochelate *III*-I have been completely assigned by homonuclear decoupling experiments (Supplementary Material). Large upfield shifts are noted for H2′ (0.08 ppm) and H3′ (0.10 ppm) signals for *III*-I relative to 5′-ITP. This may be a result of ring current from the base, which is predicted to be in a *syn* orientation (see below). Although *I*-I appears only as a minor product in the early stages of the reaction, we detect a small shift (0.04 ppm downfield) only for the H3′ signal. There are no detectable shifts of the other nonanomeric ribose protons for *I*-I although the shifts of the H2′ signal could be obscured by the HDO signal.

Pseudorotation analysis[42] for normal N ↔ S conformational equilibrium (see scheme) of the sugar indicates that the sum $^3J_{1'2'} + {}^3J_{3'4'}$ (10.5 ± 1 Hz), $\sum$, should be reasonably independent of the position of the equilibrium.[39] We observe the $\sum$ = 9.45 and 10.13 Hz for ITP and *III*-ITP, respectively. This similarity indicates that, at least for triphosphate macrochelates, the ribose ring can adopt more or less "normal" N and S configurations. The values of $^3J_{1'2'}$ and $^3J_{3'4'}$ change from 5.80 and 3.65 Hz to 5.21 and 4.92 Hz, respectively, upon formation of *III*-I from 5′-ITP, indicating a slight shift toward the N conformer on coordination of 5′-ITP.[39] The conformations about the C4′–C5′ and the C5′–O5′ bonds can be analyzed in terms of the percent gauche–gauche (% *gg*) and the percent gauche′–gauche′ (% *g′g′*), respectively (see Scheme I). These percentages are normally high (>40%),[41] with the remaining conformers distributed between *gt* and *tg* and between *g′t′* and *t′g′*, respectively. The population of *gg* and *g′g′* rotamers can be determined by using the sum rules[40]

$$\% gg = (13.3 - \sum 4'5')/9.7 \quad (1)$$

$$\% g'g' = (23.9 - \sum 5'P)/18.9 \quad (2)$$

where $\sum 4'5' = {}^3J_{4'5'} + {}^3J_{4'5''}$ and $\sum 5'P = {}^3J_{5'P} + {}^3J_{5''P}$. Both % *gg* and % *g′g′* increase upon formation of *III*-I from ITP. This

Scheme I

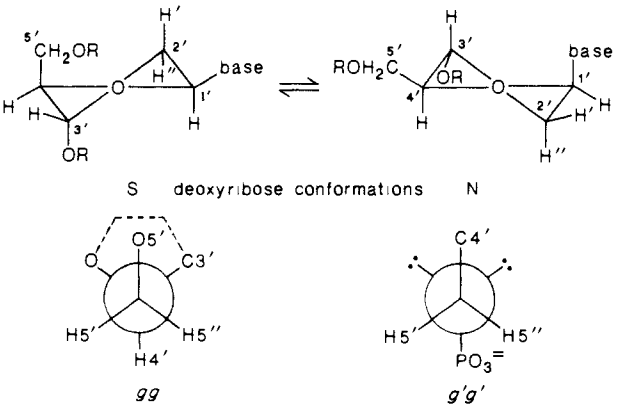

trend is consistent with models and molecular mechanics calculations (see below). Also consistent with these observations is the large increase from 2.0 to 3.2 Hz in the value of $^4J_{4'P}$ for *III*-I compared with ITP (Figure 2). Extrapolation of the 4′P coupling constant to a pure *gg*, *g′g′* configuration has yielded values from 3.0 to 3.7 Hz, with a mean value of 3.3 Hz.[40]

***cis*-$Pt(ND_2CH_3)_2$(5′-dIMP-*N7*,α*PO*) Ribose Conformations.** Complete coupling constants for *cis*-$Pt(ND_2CH_3)_2$(5′-dIMP-*N7*,α*PO*) are given in the Supplementary Material. For this species, it should be noted that Pt binding in a cis manner to the N7 and αPO constrains the ribose ring to an unusual conformation and makes an analysis like that above unreliable.[43] Application of eq 1 and 2 to this system, however, reveals an even stronger tendency for a *gg*, *g′g′* conformation about the C4′–C5′ and C5′–O5′ bonds than determined for *III*-I. The value of $^4J_{4'\alpha P}$ (3.2 Hz), identical with that of *III*-I, confirms a strong preference for the *gg*, *g′g′* conformation (see above).[40,44] The % *gg* (36) and % *g′g′* (70) calculated for 5′-dIMP are similar to those previously reported for 5′-dGMP.[41]

Comparison of Chelates Involving α, β, or γ PO Coordination: Molecular Mechanics Studies. Refinement of the initial models for *N7*,*PO* macrochelated 6-oxopurine nucleotide phosphates revealed in all cases a close contact (2.9 Å) between O6 of the purine and one of the coordinated amine ligands. Hydrogen bonds between these moieties have been reported previously[33] and therefore this interaction was modelled explicitly as a hydrogen bond in all calculations.

***cis*-$Pt(NH_3)_2$(5′-GTP-*N7*,γ*PO*) and *cis*-$Pt(NH_3)_2$(5′-dGTP-*N7*,γ*PO*).** Strain energies were calculated for the three isomers of macrochelated 5′-GTP in which the α, β, and γ phosphate groups are coordinated. Typical results are listed in Table II and the Supplementary Material. The γ isomer gives the lowest strain energy and therefore, on the basis of steric factors alone, it is the

(43) Before drawing conclusions on the nucleotide conformational states in Pt–nucleotide macrochelate complexes using parameters derived empirically from nucleotides, we must consider at least three points. First, although an N ↔ S equilibrium adequately describes the situation for poly- and mononucleotides, the additional constraint associated with macrochelate formation could tend to change the lowest energy conformations. For example, models and MM calculations (see text) reveal that formation of *cis*-$Pt(NH_3)_2$(5′-NMP-*N7*,*PO*) macrochelates tends to hold the C1′–N9 and C4′–C5′ bonds into near-axial positions. Pure N and S conformers require that one of these bonds be equatorial and the other axial,[39-41] depending on the conformer. Second, contrary to the case of mononucleotides,[40,41] rotation about the C4′–C5′ and/or C5′–O5′ bonds should be hindered in these macrochelates. This hindrance may lead to the observation of "conformationally pure" species about these bonds. Third, the empirical Karplus equations derived from the nucleotides do not account for the electronegativity effects of Pt binding to N7 and PO. For 5′-NTPs, where γ phosphate coordination is observed, we expect little influence on the conformations derived from coupling constants on the 5′ side of the sugar, whereas the electronegativity effect may be larger for 5′-NMP macrochelates coordinated through the α phosphate.[44]

(44) In an effort to determine the effect of charge withdrawal on $\alpha^{31}P$–^1H coupling constants, we studied the effect of protonation. The value of $^4J_{4'P}$ of 5′-dIMP increased with decreasing pH. Values of 0.85, 1.30, and 1.55 Hz were observed at pH 7.7, 6.5, and 4.8, respectively. There was no detectable change in the values of $^3J_{5'P}$ and $^3J_{5''P}$ over this pH range.

Table II. Strain Energies and Conformational Parameters for Macrochelate Nucleotide Complexes

conformer	energy (kJ mol^{-1})	P (deg)	τ_m (deg)	χ (deg)
	cis-Pt(NH_3)$_2$(5′-GTP-*N7*,γ*PO*)			
N,syn	63.6	346	39.4	153.5
N,anti	76.1	353	36.7	5.0
S,syn	64.8	189	34.3	176.8
S,anti	76.5	175	37.7	63.2
	cis-Pt(NH_3)$_2$(5′-GTP-*N7*,β*PO*)			
N,syn	68.9	332	38.3	119.9
	cis-Pt(NH_3)$_2$(5′-GTP-*N7*,α*PO*)			
N,syn	72.7	327	31.7	98.5
S,syn	81.3	205	36.9	110.2
	cis-Pt(NH_3)$_2$(5′-GMP-*N7*,α*PO*)			
N,syn	58.2	330	35.2	101.9
N,anti	56.9	335	41.3	−25.0
S,syn	67.8	208	35.7	111.7
S,anti	62.2	197	33.7	−13.1

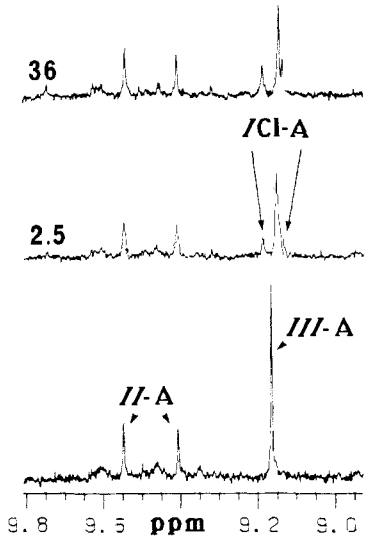

Figure 7. Effect of added Cl^- on the ^1H NMR spectrum (aromatic region) of an "equilibrated" mixture of 10 mM 5′-ATP and 10 mM *cis*-Pt(ND_2CH_3)$_2$(OD_2)(OD) at pH 6, 25 °C. 1.0 M NaCl was added to the sample to make final [Cl^-] 0.10 M shortly after recording the bottom trace. Spectra were then recorded at the times indicated (h). No further changes were observed after 36 h. Note two H8 signals for /Cl-A indicating restricted rotation. See text for spectral assignments and conditions.

isomer expected. A significant preference for the syn orientation of the purine over the anti results primarily from unfavorable interactions between the purine and the sugar in the latter case. There is a slight preference for the N conformation of the sugar over the S (62:38 at 25 °C). The proportion of the N conformer increases when compared to the free nucleotide triphosphate for which a ratio of 43:57 is predicted. The results for the 5′-dGTP complex are similar with a slightly increased preference for the N conformer (65:35). This result is surprising, since in the case of free 5′-dGTP the predicted N:S ratio is 25:75. Thus, in both cases an increased preference for the N conformer is expected for the chelates. The minimum energy sugar conformations are closer to C'_2 exo(N) and C'_3 exo(S) than to the more usual C'_3 endo and C'_2 endo, respectively.[39]

A view of the minimum energy (N, syn) conformation for *cis*-Pt(NH_3)$_2$(5′-GTP-*N7*,γ*PO*) is shown in Figure 8. The purine lies roughly perpendicular to the coordination plane and the sugar is nearly parallel to the coordination plane. The orientation of the purine is close to a normal syn, χ is 154° for N and 177° for S, compared to the idealized 180°. The conformation of the sugar phosphate linkage is *gg*, *g′g′*.

***cis*-Pt(NH_3)$_2$(5′-GTP-*N7*,α*PO*).** In contrast to the results for γ-coordinated 5′-GTP, those for the α-coordinated isomer indicate

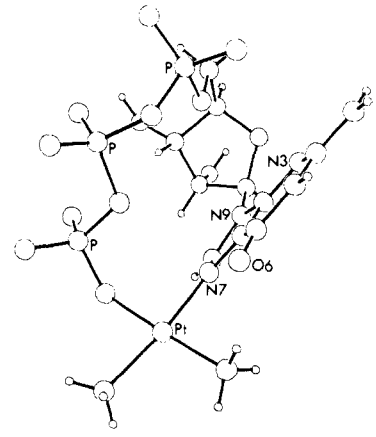

N,syn-cisPt(NH3)2(5'GTP,N7,γPO)

Figure 8. ORTEP plot of the N,syn conformer of *cis*-Pt(NH_3)$_2$(5′-GTP-*N7*,γ*PO*). Drawing based on minimized structure as described in the text.

unusual conformational properties for the sugar ring. These predicted geometries are similar to those to be described next for the 5′-GMP chelates. The S sugar conformation is significantly destabilized with respect to the N conformation.

***cis*-Pt(NH_3)$_2$(5′-GMP-*N7*,α*PO*) and *cis*-Pt(NH_3)$_2$(5′-dGMP-*N7*,α*PO*).** Final calculated strain energies for both *cis*-Pt(NH_3)$_2$(5′-GMP-*N7*,α*PO*) and *cis*-Pt(NH_3)$_2$(5′-dGMP-*N7*,α*PO*) are given in Table II and the Supplementary Material. In both complexes there is no clear preference for one particular conformation. Since the results for the two complexes are so similar, discussion will be centered on the ribose species.

The most stable geometry for *cis*-Pt(NH_3)$_2$(5′-GMP-*N7*,α*PO*) (Figure 9) has an N sugar conformation and the anti orientation of the purine with respect to the sugar. Inspection of this model reveals no highly strained bond lengths or angles, suggesting that formation of the *N7*,α*PO* coordinated macrochelate is sterically feasible. The sugar conformation is, however, somewhat different from that normally observed.[39] The pseudorotation angle, 335°, indicates a conformation close to C'_2 exo but distorted toward C'_1 endo. The S sugar conformations are also unusual being close to C'_3 exo. Considering only the anti purine conformation, an 89:11 preference for the N conformation is predicted. This ratio represents a large change from that expected for the free ligand (43:57). Thus, both the sugar geometry and the conformational preferences are altered by formation of the macrochelate.

In the anti conformation, a close contact is observed between N3 of the purine and H2′ of the sugar. In the case of the most stable geometry (N,anti), this distance is only 2.45 Å.

The barrier to N ↔ S conformational interconversion was estimated to be about 15 kJ mol^{-1} and that to syn ↔ anti interconversion to be at least 60 kJ mol^{-1}. Thus, the former process would be occurring faster than the NMR time scale and the latter considerably more slowly than this time scale, if at all.

Discussion

Spectroscopic Characterization of and Principles Governing Formation of *cis*-PtA_2 Nucleotide Complexes. The observations in this study with purine 5′-NTPs are totally consistent with previous definitive studies of complex formation of *cis*-PtA_2 species with purine 5′-NMPs.[3-12,18-20] Combining results from this study with those from previous studies, we can state some general guidelines for purine species: (a) bis complexes are formed readily and can best be avoided with 5′-NXPs by the presence of an excess of Pt complex; (b) adenine nucleotides form *N1*,*N7* bridge oligomers of polymeric products with excess Pt whereas 6-oxopurine nucleosides and nucleotides form such species appreciably only with large excesses of Pt reagent, usually under forcing conditions; (c) bis complexes have *upfield* shifted H1′ signals, with respect to the nucleotide; (d) for unhindered *cis*-PtA_2, bis complexes of 5′-GXP and 5′-IXP are in rapid rotation about the Pt–*N7* bond whereas bis 5′-AXP complexes exhibit hindered rotation; (e) mono

adducts have downfield shifted signals relative to nucleotides; (f) at a given pH, ^{31}P signals of base adducts are shifted little compared to the free nucleotide; (g) such adducts exhibit large ^{31}P shift dependence on pH similar to the free nucleotide; (h) when the phosphate group coordinates, a large downfield shift of the ^{31}P signal of the coordinated phosphate group is observed; (i) the shift, in this latter case, is not very pH dependent; (j) such phosphate group coordination is relatively unfavorable for 5′-NMP but is relatively favorable for 5′-NTP; (k) for 5′-NTPs, macrochelates can be observed under conditions where other species (e.g., bis complexes) are favored with 5′-NMPs; (l) the conformation of the ribose sugar generally has more N character compared to the free nucleotide in *N7* coordinated adducts; and (m) in *N7,PO* chelate structures, particularly 5′-NMPs, the ribose conformational change is greater than that for the *N7* adducts.

Serious misassignments of structures and misinterpretation of spectra have resulted from a failure to take all of the above points into account. We feel it is unnecessary to provide a detailed criticism of the two recent studies[16,17] which have incorrectly interpreted the products and spectral characteristics of 5′-AXP Pt complexes. Rather, we have presented strong experimental evidence here and previously[19,20] for the nature of these 6-oxo- and 6-aminopurine 5′-NXP complexes. This evidence is consistent with previous definitive literature from this and other laboratories.[3,8-12,18-20]

Prediction of Molecular Mechanics Calculations and Comparison with NMR Results. Triphosphate Complexes: Analysis of the NMR spectra of macrochelated triphosphate nucleotides suggests that their conformational preferences are not greatly altered by chelation. An increased preference for *gg* and *g′g′* orientations in the sugar to phosphate linkage is the major observable change. The molecular mechanics calculations produced the *gg* and *g′g′* orientations in accord with this observation, but other orientations cannot be ruled out since they were not explicitly investigated. The H1′–C1′–C2′–H2′ coupling constants suggest a small increase in the preference for the N conformation of the sugar ring. This is also in accord with the molecular mechanics calculations which predict an N:S ratio of 62:38 for the 5′-GTP macrochelated case and 43:57 for the free nucleotide phosphate case.

The molecular mechanics calculations predict a close to 100% preference for the syn orientation of the purine over the anti orientation. No direct evidence for this stereospecificity could be obtained from the NMR spectral data, but it is *not* inconsistent with that prediction.

Monophosphate Complexes: The results for the 5′-NMP macrochelates are in contrast to those for the triphosphate since the NMR spectra indicate large changes in conformational preferences and geometry on chelation. An almost exclusive preference for *gg* and *g′g′* orientations in the sugar-to-phosphate linkage is indicated by the NMR data.[20] Indeed, the *gt* conformation for N,anti-*cis*-Pt$(NH_3)_2$(5′-GMP-*N7,αPO*) was calculated to be much less (>10 kJ mol^{-1}) stable than the *gg* conformation.

A number of aspects of the NMR data suggest a strong preference for an N sugar conformation and, further, indicate that this conformation is an unusually distorted one.[20] The molecular mechanics calculations accord well with these NMR results and indicate 98:20 and 89:11 preferences for N in the syn and anti cases, respectively. Also, the minimum energy N conformations in these cases have unusual geometries; the pseudorotation parameters (*P*), 330° and 335°, respectively, indicate $^1_2$T conformations, roughly midway between C'_1 endo and C'_2 exo.

Molecular mechanics calculations indicated a barrier of more than 60 kJ mol^{-1} to syn-to-anti conformational interconversion. A barrier of this height suggests that if both conformers were present in solution then individual peaks in the NMR spectra would be observed for each species. The calculations show that the syn and anti conformers have comparable energies, at least for the case of the N conformer, and therefore predict a mixture of the two. However, the spectra clearly indicate the presence of only one conformer. The large downfield shift (0.4 ppm) of the H2′ signal suggests a positioning of the proton very near N3 of the purine.[20] Such a position is only consistent with the anti

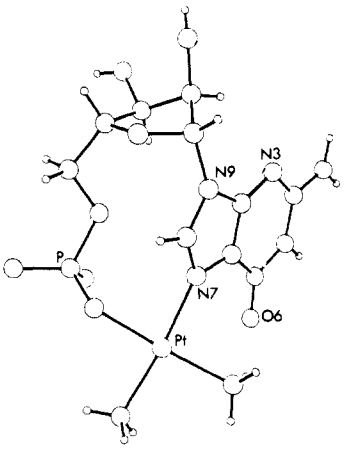

N,anti-cisPt(NH3)2(5'GMP,N7,αPO)

Figure 9. ORTEP plot of the N,anti conformer of *cis*-Pt$(NH_3)_2$(5′-GMP-*N7,αPO*). (See Figure 8 caption.)

conformation and, indeed, a separation between N3 and H2′ of only 2.45 Å is observed in the energy minimized N,anti structure. Clearly then, the NMR data are most consistent with the N,anti conformation calculated to have the lowest strain energy. The exclusive occurrence of the anti conformer might be due to kinetic factors. The size of the barrier to syn-to-anti interconversion is sufficiently large to prevent subsequent interchange on a reasonable time scale.

Macrochelates with Labile, Biologically Relevant Metal Ions. Metal–nucleotide complexes have importance outside the area of Pt anticancer drugs. These species are of fundamental chemical interest exhibiting a rich coordination chemistry.[4,22-27] Furthermore, metal–nucleotide complexes are often, if not always, the species involved in nucleotide biochemistry.[4,22-27] However, the complexes of interest involve labile metal ions such as Mg^{2+}, Ca^{2+}, and Mn^{2+}. The latter is often substituted for the two former cations because of its useful probe characteristics.[26] Indeed, one of the first applications of NMR spectroscopy to a biological problem involved a study of metal–nucleotide interactions.[45]

As mentioned above, macrochelates have frequently been postulated in these systems.[22-24,28] However, there are no X-ray structures of such species, although the evidence in solution, involving formation constants as well as VIS and NMR spectroscopic changes, is quite strong.[23,24,28] Nevertheless, it is difficult to prove with labile species that both the base and the phosphate are bound simultaneously to the metal center and often it is not clear which phosphate group(s) of a 5′-NTP is (are) bound to the metal center.

From this study, it *is* clear that γPO_4 coordination to a site cis to the N7 coordination site is quite favored. Indeed, even 100 mM Br^- is able to displace only partially the coordinated phosphate group. In studies with other metal species where macrochelates have been clearly identified, the percentage of macrochelate to exclusively phosphate bound species appears to depend on the affinity of the metal for N. Since Pt(II) has a high preference for N over O donors, this metal center is at or near the N preference extreme of the series. However, despite the relatively low affinity of Pt(II) for O donors, the macrochelate is formed. Therefore, the results indirectly support reported evidence for 5′-NTP macrochelates with other metals such as Ni(II), which have a relatively lower preference for N over O donors.[28]

In contrast to the data with 5′-NTP and 5′-NDP species, good evidence for macrochelates with 5′-NMPs is rare.[4,28] Indirect chelates—in which a coordinated H_2O forms a H bond to an uncoordinated phosphate group—are frequently observed in X-ray structures.[4,46,47] Stability constant comparisons suggest that

(45) Cohn, M.; Hughes, T. R., Jr. *J. Biol. Chem.* **1962**, *237*, 176.
(46) Miller, S. K.; Van Derveer, D. G.; Marzilli, L. G. *J. Am. Chem. Soc.* **1985**, *107*, 1048.
(47) Swaminathan, V.; Sundaralingam, M. *CRC Crit. Rev. Biochem.* **1979**, *6*, 245.

5'-AMP forms an *N7,αPO* chelate with Ni(II),[28] but it is difficult to allow for the consequences of indirect chelation. We believe that our recent study with Pt(II) compounds unambiguously establishes such a direct *N7,αPO* chelate.[20] Indeed, a second unambiguous class of *N7,αPO* chelates was recently reported by Marks and co-workers.[48] The neutral complex, $Mo(C_5H_5)_2$-(5'-AMP-*N7,αPO*), is stable enough to be isolated and characterized as a monomer by cryoscopic and mass spectral methods. Its NMR spectral characteristics are consistent with features discussed here. It is also interesting to point out that $Mo(C_5H_5)_2Cl_2$ is an antineoplastic agent.

(48) Kuo, L. Y.; Kanatzidis, M. G.; Marks, T. J. *J. Am. Chem. Soc.* **1987**, *109*, 7207.

These experiments and the molecular mechanics calculations suggest that macrochelates are sterically and energetically feasible. Clearly, the intermediacy of such macrochelates in nucleotide biochemistry deserves continued consideration.

Acknowledgment. Support of this study by NIH Grant GM29222 and a loan of K_2PtCl_4 from Matthey-Bishop, Inc., are greatly appreciated. The NMR instrumentation and the computers employed in this study were obtained with partial support from NSF and NIH, respectively.

Supplementary Material Available: Tables of NMR spectral data and strain energies and conformational parameters for 5'-dNXP complexes (2 pages). Ordering information is given on any current masthead page.

Comparison of Variable-Temperature ^1H NMR Spectra of Five-Coordinate High-Spin ($S = {}^5/_2$) Iron(III) Porphyrins and Chlorins

M. J. Pawlik, P. K. Miller, E. P. Sullivan, Jr., M. A. Levstik, D. A. Almond, and S. H. Strauss*[1]

Contribution from the Department of Chemistry, Colorado State University, Fort Collins, Colorado 80523. *Received June 1, 1987*

Abstract: Variable-temperature ^1H NMR spectra are reported for five different five-coordinate high-spin ($S = {}^5/_2$) iron(III) chlorin complexes. The complexes are Fe(TPC)X ($X^- = Cl^-$, $OTeF_5^-$) and Fe(OEC)X ($X^- = Cl^-$, $OTeF_5^-$, NCS^-), where TPC = tetraphenylchlorinate dianion and OEC = octaethylchlorinate dianion. For completeness, variable-temperature spectra are also reported for the five homologous porphyrin complexes, although with one exception, Fe(OEP)(NCS), these porphyrin data have been reported by others. Spectra and Curie plots for the two classes of complexes are compared and spectral characteristics that are unique to chlorins are discussed. Our data show that the various types of pyrrole protons in the TPC complexes and the various types of pyrrole methylene protons in the OEC complexes exhibit a large range of isotropic shifts, ~30 ppm at ~300 K. The average temperature dependence of the resonances (i.e., Curie plot slopes) is similar to the temperature dependence of the resonance(s) for porphyrin protons in chemically similar positions. For both sets of chlorin complexes, pyrroline proton or methylene proton isotropic shifts are substantially smaller than pyrrole isotropic shifts, while pyrroline proton or methylene proton line widths are larger than pyrrole proton line widths. Large deviations in Curie plot $1/T = 0$ intercepts from diamagnetic chemical shifts are observed for many of the chlorin proton resonances. This behavior has been observed for all paramagnetic iron(II,III) hydroporphyrins studied to date. The different axial ligands greatly influence the range of isotropic shifts for the pyrrole protons or pyrrole methylene protons for a given chlorin and the temperature dependence (Curie plot slopes and intercepts) of the pyrroline protons for the TPC complexes.

Our interest in the chemical,[2-5] structural,[4,6,9] and magnetic[2,6-9] properties of iron hydroporphyrins[10] (chlorins and isobacteriochlorins) stems from their occurrence in a wide variety of heme proteins and enzymes.[11,12] Magnetic properties are of fundamental importance to biochemists who isolate and work with heme proteins, because data such as EPR and Mössbauer spectra, paramagnetic ^1H NMR spectra, and effective magnetic moments have been used to elucidate the molecular and electronic structure of

(1) Alfred P. Sloan Fellow, 1987-1989.
(2) Stolzenberg, A. M.; Strauss, S. H.; Holm, R. H. *J. Am. Chem. Soc.* **1981**, *103*, 4763.
(3) Strauss, S. H.; Holm, R. H. *Inorg. Chem.* **1982**, *21*, 863.
(4) Strauss, S. H.; Silver, M. E.; Ibers, J. A. *J. Am. Chem. Soc.* **1983**, *105*, 4108.
(5) Strauss, S. H.; Thompson, R. G. *J. Inorg. Biochem.* **1986**, *27*, 173.
(6) Strauss, S. H.; Silver, M. E.; Long, K. M.; Thompson, R. G.; Hudgens, R. A.; Spartalian, K.; Ibers, J. A. *J. Am. Chem. Soc.* **1985**, *107*, 4207.
(7) Strauss, S. H.; Pawlik, M. J. *Inorg. Chem.* **1986**, *25*, 1921.
(8) Strauss, S. H.; Long, K. M.; Majerstadt, M.; Gansow, O. A. *Inorg. Chem.* **1987**, *26*, 1185.
(9) Strauss, S. H.; Pawlik, M. J.; Skowyra, J.; Kennedy, J. R.; Anderson, O. P.; Spartalian, K.; Dye, J. L. *Inorg. Chem.* **1987**, *26*, 724.
(10) (a) The fully unsaturated porphyrin macrocycle contains 11 conjugated double bonds. A variety of compounds are known in which the macrocycle porphyrin skeleton is retained while one or more double bonds are removed. These compounds are formally derived from porphyrins by hydrogenation and are, therefore, commonly called hydroporphyrins. Note that the generic term hydroporphyrin refers to compounds in which the substituent(s) added across the double bond(s) are hydrogen atoms, alkyl or substituted-alkyl groups, alkylidene groups, or oxygen or sulfur atoms: Scheer, H. In *The Porphyrins*; Dolphin, D., Ed.; Academic Press: New York, 1978; Vol. II, pp 1-44. Scheer, H.; Inhoffen, H. H. *Ibid.* pp 45-90. (b) Chlorins, which contain 10 conjugated double bonds, are porphyrins that have interrupted conjugation at vicinal C_b atoms of a single pyrrole ring. The affected ring is called a pyrroline ring. Isobacteriochlorins, which contain nine conjugated double bonds, are porphyrins that contain two adjacent pyrroline rings.

(11) (a) Andersson, L. A.; Loehr, T. M.; Lim, A. R.; Mauk, A. G. *J. Biol. Chem.* **1984**, *259*, 15340. (b) Koland, J. G.; Miller, M. J.; Gennis, R. B. *Biochemistry* **1984**, *23*, 445. (c) Miller, M. J.; Gennis, R. B. *J. Biol. Chem.* **1985**, *260*, 14003. (d) Timkovich, R.; Cork, M. S.; Gennis, R. B.; Johnson, P. Y. *J. Am. Chem. Soc.* **1985**, *107*, 6069. (e) Kim, C.-H.; Hollocher, T. C. *J. Biol. Chem.* **1984**, *259*, 2092. (f) Timkovich, R.; Cork, M. S.; Taylor, P. V. *Ibid.* **1984**, *259*, 1577. (g) Timkovich, R.; Cork, M. S.; Taylor, P. V. *Ibid.* **1984**, *259*, 15089. (h) Sibbett, S. S.; Hurst, J. K. *Biochemistry* **1984**, *23*, 3007. (i) Ikedo-Saito, M.; Prince, R. C. *J. Biol. Chem.* **1985**, *260*, 8301. (j) Babcock, G. T.; Ingle, R. T.; Oertling, W. A.; Davis, J. C.; Averill, B. A.; Hulse, C. L.; Stufkens, D. J.; Bolscher, B. G. J. M.; Wever. R. *Biochim. Biophys. Acta* **1985**, *828*, 58. (k) Bolscher, B. G. M.; Wever, R. *Ibid.* **1984**, *788*, 1. (l) Park, C. M.; Nagel, R. L. *New Engl. J. Med.* **1984**, *310*, 1579. (m) Timkovich, R.; Vavra, M. R. *Biochemistry* **1985**, *24*, 5189. (n) Timkovich, R. *Ibid.* **1986**, *25*, 1089. (o) Chatfield, M. J.; La Mar, G. N.; Balch, A. L.; Lecomte, J. T. J. *Biochem. Biophys. Res. Commun.* **1986**, *135*, 309. (p) Chatfield, M. J.; La Mar, G. N.; Lecomte, J. T. J.; Balch, A. L.; Smith, K. S.; Langry, K. C. *J. Am. Chem. Soc.* **1986**, *108*, 7108.
(12) (a) Christner, J. A.; Munck, E.; Kent, T. A.; Janick, P. A.; Salerno, J. C.; Siegel, L. M. *J. Am. Chem. Soc.* **1984**, *106*, 6786. (b) Chang, C. K. *J. Biol. Chem.* **1985**, *260*, 9520. (c) Cline, J. F.; Janick, P. A.; Siegel, L. M.; Hoffman, B. M. *Biochemistry* **1986**, *25*, 7942.

0002-7863/88/1510-3007$01.50/0